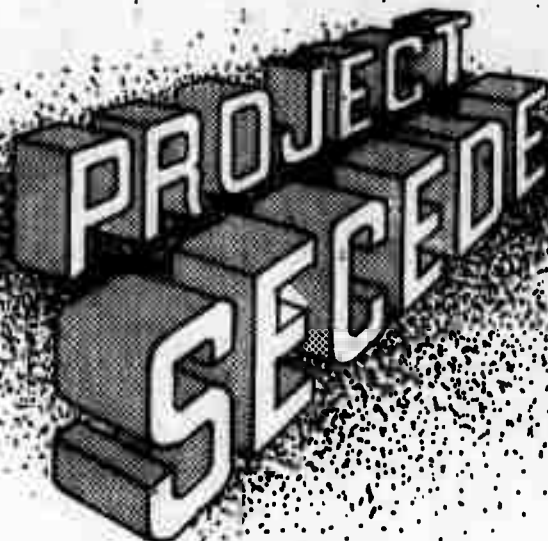


RADC-TR-72-130
Technical Report
April 1972



Prepared By
Rome Air Development Center
Air Force Systems Command
Griffiss Air Force Base, New York 13440

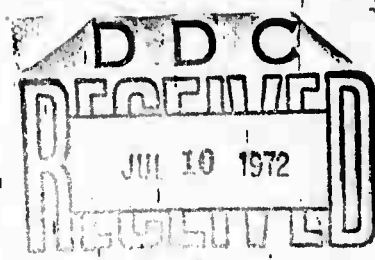
AD 745572



SECEDE II STRIATION ANALYSIS

EG&G, Bedford Division

Sponsored by
Defense Advanced Research Projects Agency
ARPA Order No. 1057



Approved for public release;
distribution unlimited.

The views and conclusions contained in this document are those of the authors and should not be interpreted as necessarily representing the official policies, either expressed or implied, of the Defense Advanced Research Projects Agency or the U. S. Government.

Reproduced by
NATIONAL TECHNICAL
INFORMATION SERVICE
U S Department of Commerce
Springfield VA 22151

X 72-574

**BEST
AVAILABLE COPY**

DOCUMENT CONTROL DATA - R & D

(Security classification of title, body of abstract and indexing annotation must be entered when the overall report is classified)

1. ORIGINATING ACTIVITY (Corporate author) EG&G, Bedford Division Crosby Drive Bedford, Massachusetts 01730		2a. REPORT SECURITY CLASSIFICATION Unclassified	
		2b. GROUP	
3. REPORT TITLE SECEDE II Striation Analysis			
4. DESCRIPTIVE NOTES (Type of report and inclusive dates) Semi-Annual Technical Report July 1971 - January 1972			
5. AUTHOR(S) (First name, middle initial, last name) Harold J. Linnerud Lawrence H. Leonard Edward P. Marram			
6. REPORT DATE April 1972	7a. TOTAL NO. OF PAGES 38	7b. NO. OF REFS -	
8a. CONTRACT OR GRANT NO. F30602-71-C-0015	8b. ORIGINATOR'S REPORT NUMBER(S)		
9. PROJECT NO. ARPA Order No. 1057	9b. OTHER REPORT NO(S) (Any other numbers that may be assigned this report) RADC-TR-72-130		
10. DISTRIBUTION STATEMENT Approved for public release; distribution unlimited.			
11. SUPPLEMENTARY NOTES Monitored by: Richard Schneible RADC/OCSE Griffiss AFB, N.Y. 13440		12. SPONSORING MILITARY ACTIVITY Advanced Research Project Agency 1400 Wilson Blvd. Arlington, VA 22209	
13. ABSTRACT To support SECEDE II data analysis and interpretation, EG&G (Bedford Division) is analyzing photographic data from the Spruce Event. Fourier analysis of digitized data frames will produce power spectra, auto-correlation functions, and other such data as is appropriate for event interpretation and correlation. The concept of Fourier analysis is also being examined to establish the validity and usefulness of the analysis results.			

ia

14.

KEY WORDS

LINK A

LINK B

LINK C

ROLE

WT

ROLE

WT

ROLE

WT

1) Barium Release

2) Fourier Analysis

3) Power Spectra

16

SECEDE II STRIATION ANALYSIS

H. J. Linnerud
L. H. Leonard
E. P. Marram

Contractor: EG&G, Bedford Division
Contract Number: F30602-72-C-0015
Effective Date of Contract: 6 July 1971
Contract Expiration Date: 6 July 1972
Amount of Contract: \$49,800.00
Program Code Number: 2E20

Principal Investigator: Dr. H. J. Linnerud
Phone: 617 271-5804

Project Engineer: Vincent J. Coyne
Phone: 315 330-3107

Contract Engineer: Richard Schneible
Phone: 315 330-3451

Approved for public release;
distribution unlimited.

This research was supported by the
Defense Advanced Research Projects
Agency of the Department of Defense
and was monitored by Richard Schneible,
RADC (OCSE), GAFB, NY 13440 under con-
tract F30602-72-C-0015.

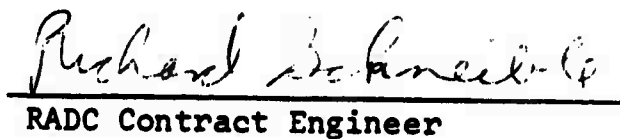
Details of illustrations in
this document may be better
studied on microfiche

IC

PUBLICATION REVIEW

This technical report has been reviewed and is approved.


RADC Project Engineer


RADC Contract Engineer

Id

ABSTRACT

To support SECEDE II data analysis and interpretation, EG&G (Bedford Division) is analyzing photographic data from the Spruce Event. Fourier analysis of digitized data frames will produce power spectra, autocorrelation functions, and other such data as is appropriate for event interpretation and correlation. The concept of Fourier analysis is also being examined to establish the validity and usefulness of the analysis results.

TABLE OF CONTENTS

<u>Section</u>		<u>Page</u>
1	INTRODUCTION	1
2	SPRUCE STRIATIONS	3
3	SOME PRELIMINARY THOUGHTS ON DATA PROCESSING FOR STRIATIONS	10
	3.1 Introduction	10
	3.2 Stationarity and Ergodicity	11
	3.2.1 Classification of Stochastic Processes	12
	3.2.2 Nonstationary Stochastics	16
	3.3 SECEDE-TYPE STRIATION DATA	18
	3.3.1 Ergodicity of $S(x)$	20
APPENDIX		
A	RADIOMETRIC INTERPRETATION OF PHOTOGRAPHIC RECORDS	28

LIST OF ILLUSTRATIONS

<u>Figure</u>		<u>Page</u>
1	Event Spruce as seen at 16 min, 5 sec from Tyndall	4
2	Event Spruce as seen at 17 min, 52 sec from Tyndall	5
3	Event Spruce as seen at 20 min, 28 sec from Tyndall	6
4	Event Spruce as seen at 23 min, 36 sec from Tyndall	7
5	Event Spruce as seen from Tyndall on T. I. C. record 71721 at 20 minutes	9
6	Classification of Stochastic Processes	12
7	Ensemble of sample functions forming random process	13
8	Examples of nonstationary data	17
9	A single feature and its transform	21
10	The addition of a second feature	22
11	The total record of randomly replicated features ...	23
12	Sample functions $x(t)$ for five examples of random processes	26

SECTION 1
INTRODUCTION

The Bedford Division of EG&G has channeled its efforts on the SECEDE program in two directions. First, it is attempting to characterize the structured environment (i. e., striations) created in a late-time barium cloud. Second, it is acquiring and correlating all such data from SECEDE I, II, and III, BIRDSEED, certain pre-SECEDE releases, and from other environments. This is a first semi-annual technical report describing some preliminary work in both of these areas.

In the first area, EG&G has been asked to proceed with a digital analysis of appropriate photography. In particular, selected frames of data from Technology International Corporation (TIC) photography are being scanned on a Mann Trichromatic Microdensitometer, and the density and/or radiance profiles generated from the scanned data are being digitally analyzed using Fourier techniques to produce power spectra, auto-covariance, and auto-correlation functions, and other such data as might prove useful.

In parallel with the analysis of photographic data, EG&G is also undertaking an examination of the applicability, validity, and limitations of such analysis. It has become apparent that members of the SECEDE community not knowledgeable in the areas of photographic data analysis, digital analysis, and Fourier techniques would find such a study of considerable interest. In particular, EG&G will attempt to examine the realistic and practical limits of such analysis work, and will attempt to give the user a basic understanding of the meaning of, and validity of, power spectra, Fourier transforms, and other such data.

In the second area, EG&G is reviewing all available SECEDE documentation and will organize pertinent information in tabular and/or matrix formulations to facilitate correlation and interpretation of results. It is currently anticipated that the results of this effort will be presented in EG&G's final report, when all available data has been acquired.

Section 2 herein presents the radiometric data which is being Fourier analyzed. Pertinent frames of data from the Spruce Event of SECEDE II are identified for analysis and radiance profiles presented. Section 3 begins the detailed examination of Fourier analysis as applied to microdensitometer data.

Appendix A contains notes prepared during the SECEDE Summer Study. These notes detail some of the assumptions, tools, and relationships used by EG&G in obtaining radiometric information from photographic data. It is reproduced here for the benefit of those members of the SECEDE community who did not receive it at the Summer Study.

SECTION 2
SPRUCE STRIATIONS

The EG&G striation analysis effort will be directed at Event Spruce. In particular, four frames of data (Table 1) will be analyzed in the Fourier domain for spatial frequency content. These frames were selected because they best bracketed the sphere and beacon track times, and because the data generated could potentially be used to correlate with the sphere and beacon data.

Table 1. Event Spruce Striation Analysis.

T. I. C. Film No. 71723

<u>Frame</u>	<u>Time (after release)</u>
146	16 min, 5 sec
164	17 min, 52 sec
185	20 min, 28 sec
193	23 min, 36 sec

The referenced frames and generated radiance profiles (across the striations) are shown in Figures 1-4. One hopes, with Fourier analysis techniques applied to the digitized radiance profile, that the small scale structure seen superimposed on the overall cloud background can be characterized in a power spectrum presentation. These profiles are currently being digitally processed; the results of the analysis will be presented in the final report.

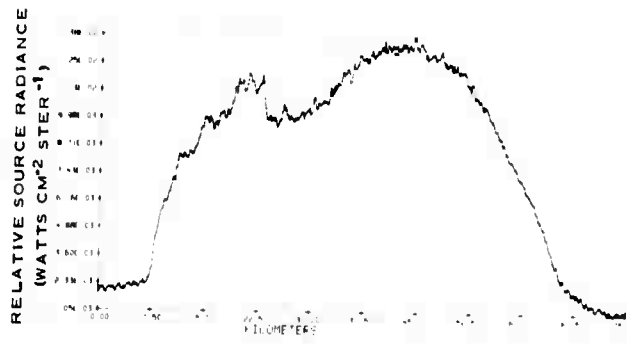
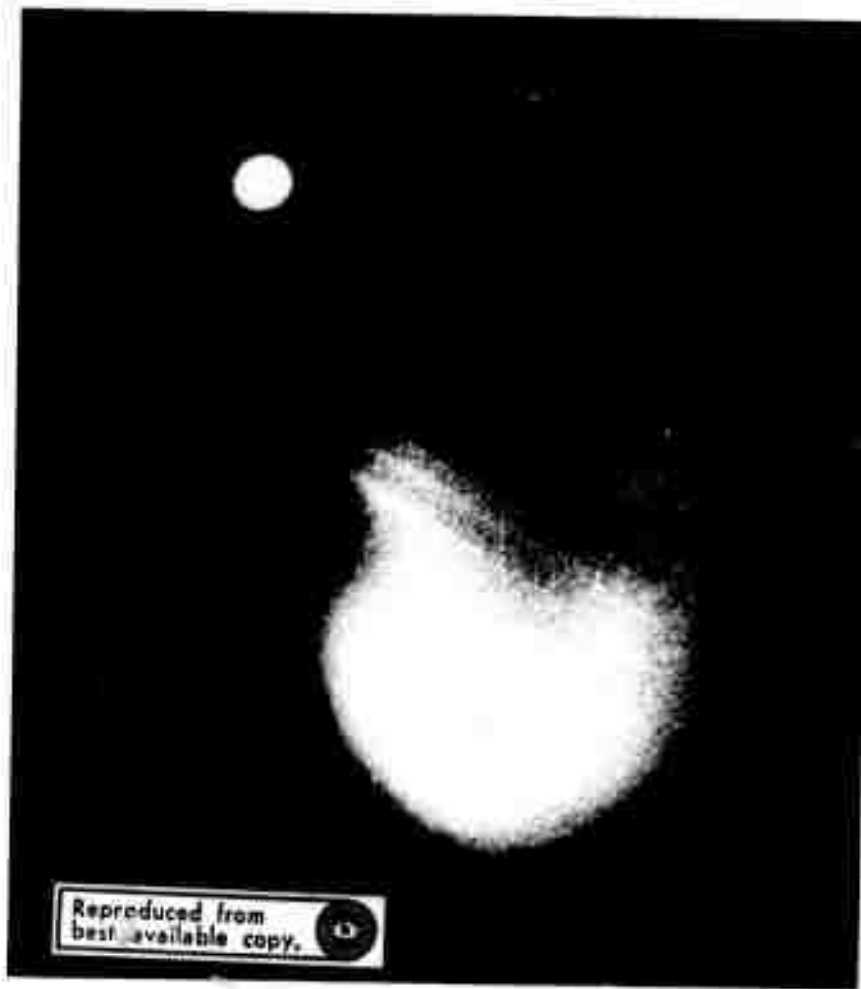


Figure 1. Event Spruce as seen at 16 min, 5 sec from Tyndall.

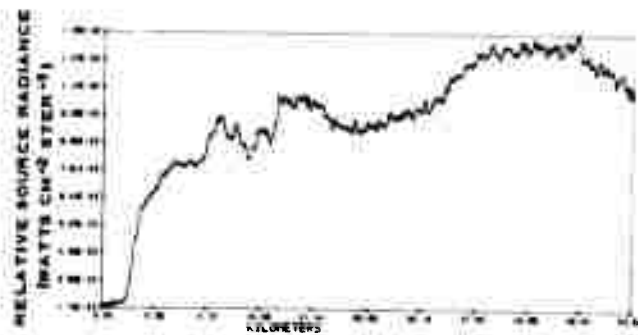


Figure 2. Event Spruce as seen at 17 min, 52 sec from Tyndall.

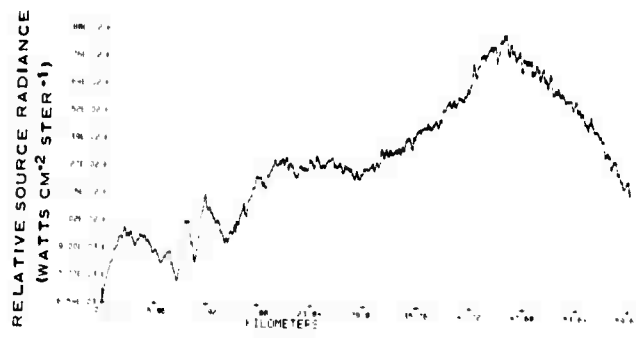


Figure 3. Event Spruce as seen at 20 min, 28 sec from Tyndall.

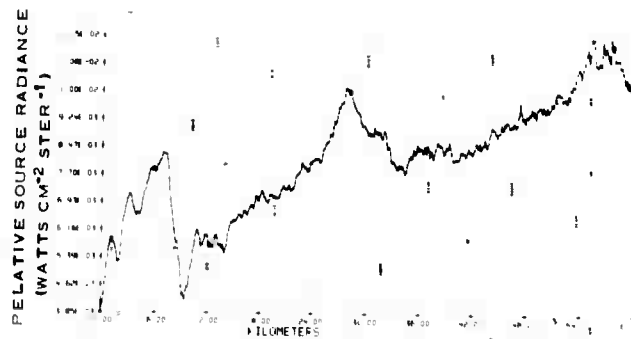


Figure 4. Event Spruce as seen at 23 min, 36 sec from Tyndall.

The Spruce ion cloud at approximately 20 minutes is shown in Figure 5 as Frame 187, from T. I. C. record 71721 (originally a color record, printed here in black-and-white). This record was exposed from Tyndall; and assuming an ROA (range along the optical axis) of 300 km, a dimensional scale was placed on the photograph to indicate relative cloud and striation dimensions.

Of particular concern here is the striated region indicated by the arrow. Are these characteristic and/or repetitive striation dimensions and spacings which can be measured from photography such as this? If not, what data can be gleaned from records such as these, and what does this data indicate about the spatial and temporal history of striations per se. Section 3 begins a detailed examination of this question and presents the implications of the answers to that question.

10



Figure 5. Event Spruce as seen from Tyndall on T. I. C. record 71721 at 20 minutes.

SECTION 3

SOME PRELIMINARY THOUGHTS ON DATA PROCESSING FOR STRIATIONS

3.1 INTRODUCTION

Shortly after the high-altitude release of barium, the ion cloud is observed to form striations - highly structured "tubes" roughly parallel to the geomagnetic field. The striations are visual/photographic. They map the local geomagnetic field, and their formation is the result of interactions between the geomagnetic field, the \vec{E} -field, ionospheric winds, and the ion cloud.

In order to interpret the available SECEDE data and to predict future data, it is necessary to describe the striations, at least statistically. A major portion of the SECEDE effort is thus directed toward developing information on the growth and formation of striations.

One part of the overall striation analysis effort is directed toward the generation of spatial frequency-domain power spectra of striated ion-cloud radiance profiles. It is generally believed that such information will assist in the assessment and interpretation of SECEDE data, although the detailed connection between the spatial frequency content of visible striations and the various signal degradations has not been established. Perhaps the connection could be established if good spatial frequency descriptions were available.

But what do we mean by "good"? Ideally, we would mean descriptions permitting an exact prediction of any future event; that is, deterministic relations or equations into which we would insert the various experimental

parameters (height of release, quantity of free barium, etc.). Those equations would then be solved to determine such characteristics as the time and location at which striations would form, their size, brightness, and distribution in space. Apparently such equations are presently beyond our grasp. In fact, the SECEDE experiments suggest that the distribution and size of striations are the result of a random physical process. If that is the case, completely deterministic equations are unattainable.

It does not matter whether the apparent randomness correctly reflects the fundamental nature of the process, is a consequence of an uncontrolled (random) systematic parameter such as the local \vec{E} -field, or simply reflects our lack of theoretical understanding of a deterministic process. Our best current theory is that the size, location, and intensity of striations are the results of a stochastic process for a given event.

What we can mean by "good" descriptions, then, are those from which an accurate statistical "prediction" of the striations which might be observed in some future event can be made. Suppose, for instance, that the radiance profiles of individual striations have the same waveform, but that amplitude and spacing are random. In that case, a good description would consist of (1) a description of that waveform, (2) an amplitude description (at least the mean amplitude), and (3) spacing statistics.

3.2 STATIONARITY AND ERGODICITY

Stochastic processes are analyzed through the examination of various ensemble averages; that is, the same experiment is repeated, in principle, an infinite number of times, and the results of each are treated as one statistical sample of the random process. However, for certain restricted classes of stochastics it is possible to obtain the desired statistics with considerably less than an infinite number of identical experiments, perhaps with as few as one.

A classification tree for stochastic processes is shown in Figure 6. Processes classified as ergodic have the property that the statistics of a single sample are identical to the ensemble statistics. In reality, we never observe a complete sample (since it's infinitely long) but rather some fraction of the complete sample which might be called the sample record. From one such record, we can obtain an estimate of the statistical parameters of the process. The accuracy of that estimate is related to the record length. That accuracy can be improved by analyzing a longer record or by combining data from shorter records.

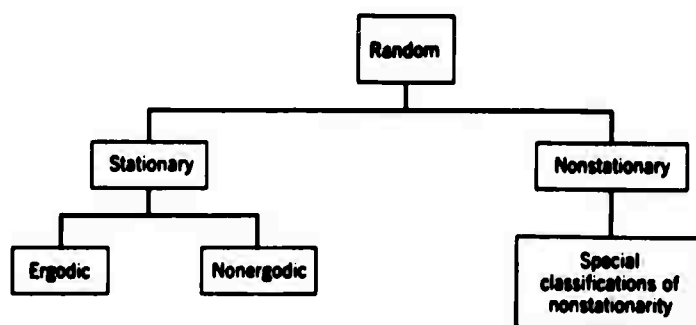


Figure 6. Classification of Stochastic Processes.

3. 2. 1 Classification of Stochastic Processes

Figure 7* shows part of an ensemble of sample records. If we read the value of x at t_1 for each record and divide by the number of records, we obtain the ensemble average, designated $\mu_x(t_1)$, at t_1 . In general, $\mu_x(t_1)$ will take on different values as t_1 is changed. In the same way, we may define the ensemble average autocorrelation function, $R_x(t_1, t_1 + \tau)$, which will generally be a function of both t_1 and τ . The equations are

*Many illustrations use "t" to denote the independent variable and x as the stochastic. The origin of most of this work is in communication theory where t is time. The reader is expected to make the appropriate mental substitutions, such as $t \rightarrow x$ and $x \rightarrow N(x)$.

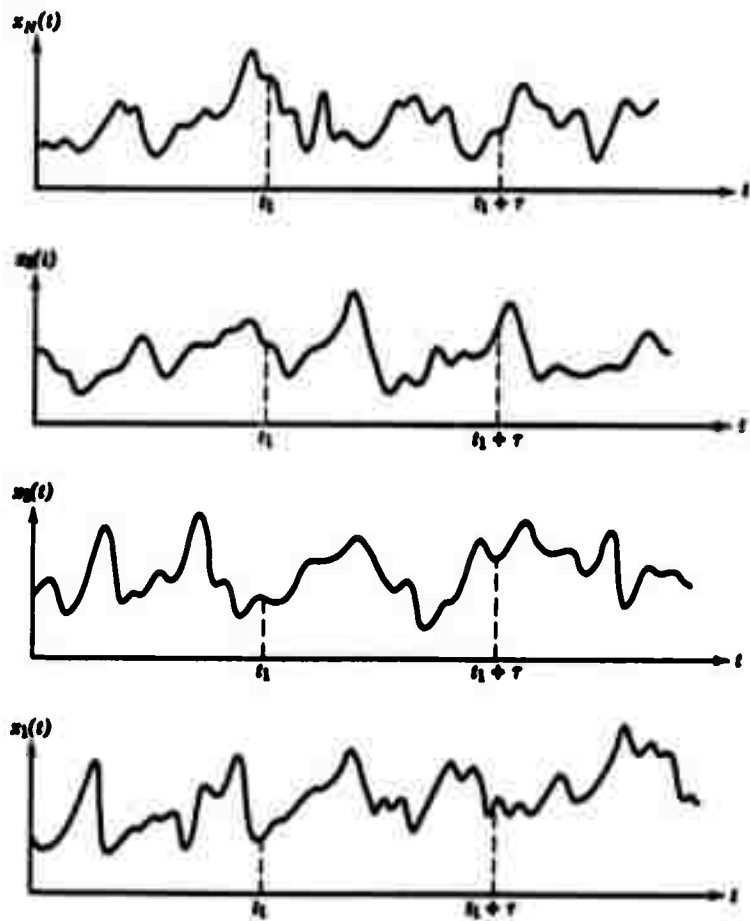


Figure 7. Ensemble of sample functions forming random process.

$$\mu_x(t_1) = \lim_{N \rightarrow \infty} \frac{1}{N} \sum_{k=1}^N x_k(t_1)$$

$$R_x(t_1, t_1 + \tau) = \lim_{N \rightarrow \infty} \frac{1}{N} \sum_{k=1}^N x_k(t_1) x_k(t_1 + \tau)$$

If these averages do, in fact, vary with the choice of t_1 , then the process is said to be nonstationary. But, if it should happen that the ensemble average and ensemble autocorrelation are independent of the choice of t_1 , the process is said to be stationary. * In that case, we may write $\mu_x(t_1) = \mu_x$ and $R_x(t_1, t_1 + \tau) = R_x(\tau)$.

It is also possible to form a mean and autocorrelation for a single sample function:

$$\mu_x(k) = \lim_{T \rightarrow \infty} \frac{1}{T} \int_0^T x_k(t) dt$$

$$R_x(\tau, k) = \lim_{T \rightarrow \infty} \frac{1}{T} \int_0^T x_k(t) x_k(t + \tau) dt$$

where k denotes the k -th sample of the (stationary) process. If both $\mu_x(k)$ and $R_x(\tau, k)$ have the same value for all k 's, then the process is said to be ergodic. In that case, the various sample averages and ensemble averages are equal; i. e., $\mu_x(k) = \mu_x$ and $R_x(\tau, k) = R_x(\tau)$.

*Strictly, if μ and R are independent of t_1 , the process is "weakly stationary". If all higher order moments and joints moments are also independent of t_1 , the process is "strongly stationary" or "strictly stationary".

The concept of stationarity relates to the ensemble averaged properties of a random process. In practice, however, data in the form of individual time-history records for a random phenomenon are frequently referred to as stationary or nonstationary. A slightly different concept of stationarity is involved here. When a single time-history record is referred to as being stationary, it is generally meant that the properties computed over short time intervals do not vary "significantly" from one interval to the next. The word "significantly" is used here to mean that observed variations are greater than would be expected, owing to normal statistical sampling variations. Hence the single sample record is stationary within itself. This concept of stationarity is sometimes called self-stationarity to avoid confusion with the more classical definition.

To clarify the idea of self-stationarity, consider a single sample record $x_k(t)$ obtained from the k-th sample function of random process $x(t)$. Assume that a mean value and an autocorrelation function are obtained by time averaging over a short interval T with a starting time of t_1 as follows.

$$\mu_x(t_1, k) = \frac{1}{T} \int_{t_1}^{t_1+T} x_k(t) dt$$

$$R_x(t_1, t_1 + \tau, k) = \frac{1}{T} \int_{t_1}^{t_1+T} x_k(t) x_k(t + \tau) dt$$

For the general case where the sample properties vary significantly as the starting time t_1 varies, the individual sample record is said to be self-nonstationary. For the special case where the sample properties do not vary significantly as the starting time t_1 varies, the sample record is said to be weakly self-stationary. If this requirement is met for all higher order moments and joint moments, the sample record is said to be strongly self-stationary.

An important point here is as follows: A sample record obtained from an ergodic random process will be self-stationary. Furthermore, sample records from most physically interesting nonstationary random processes will be self-nonstationary. Hence, if an ergodic assumption is justified (as it is for most actual stationary physical phenomena), verification of self-stationarity for a single sample record will effectively justify an assumption of stationarity and ergodicity for the random process from which the sample record is obtained.

Ergodic random processes are clearly an important class of random processes since all properties of ergodic random processes can be determined by performing time averages over a single sample function. Fortunately, in actual practice, random data representing stationary physical phenomena are generally ergodic. It is for this reason that the properties of stationary random phenomena can be measured properly, in many cases, from a single observed time-history record.

3. 2. 2 Nonstationary Stochastics

Nonstationary random processes include all random processes which do not meet the requirements for stationarity. Unless further restrictions are imposed, the properties of nonstationary random processes are generally time-varying functions which can be determined only by performing instantaneous averages over the ensemble of sample functions forming the process. In practice, it is often not feasible to obtain a sufficient number of sample records to permit the accurate measurement of properties by ensemble averaging. This fact has tended to impede the development of practical techniques for measuring and analyzing nonstationary random data.

In fact, a totally adequate methodology does not as yet exist for the analysis of all types of nonstationary data, partly because of the fact that a nonstationary conclusion is generally a negative statement specifying the lack of stationary properties, rather than defining the precise nature of the

nonstationarity. On the other hand, when a process is deemed stationary, certain positive results are known which apply to all stationary data. For nonstationary data, special techniques must be developed which apply only to limited classes of these data.

Illustrated in Figure 8 are the three basic and most important categories of nonstationary data: (a) time-varying mean value, (b) time-varying mean square value, and (c) a combination of (a) and (b). As we shall see, the radiance profile of the striated ion cloud is probably nonstationary (category c); however, it may be possible to treat the striations, per se, as ergodic.

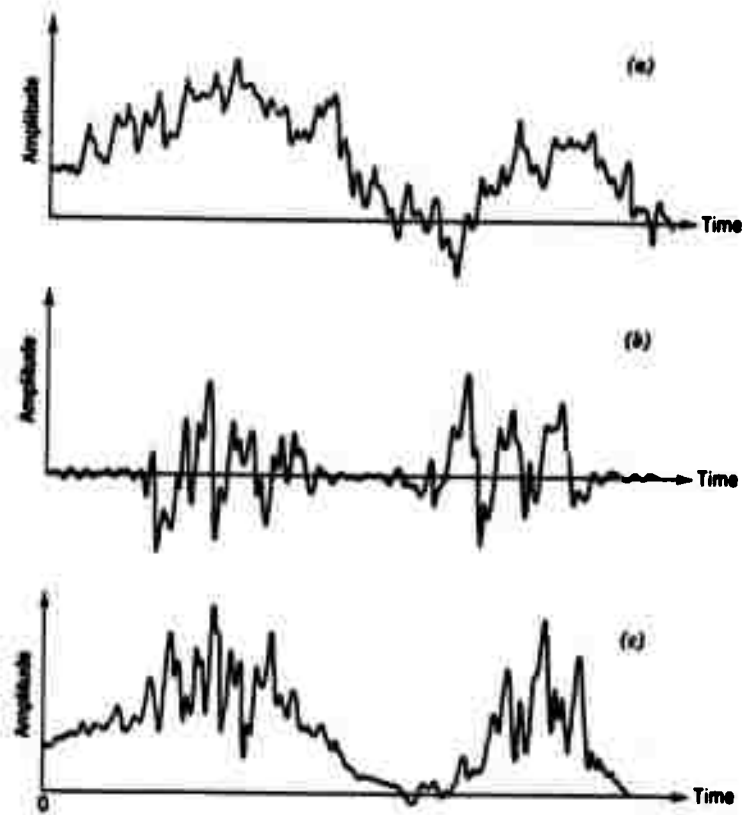


Figure 8. Examples of nonstationary data.

3.3 SECEDE-TYPE STRIATION DATA

Figures 1 through 4 contain typical radiance profiles for striated barium ion clouds. To the extent that these scans are, in fact, typical, it is evident that the ion cloud radiance profile data has a distance varying mean and mean square. (Compare with Figure 8.) The data is nonstationary (thus, nonergodic). We are not, however, particularly interested in the gross behavior of the ion cloud, nor do we care about gradation in the general sky brightness. If we could subtract these two effects* from the radiance profile, we might be left with a data record which is ergodic.

To the best of our knowledge, such a subtraction has not been attempted for SECEDE-type striation data; thus, we do not know exactly how to proceed. We are inclined to try simple procedures first, and the remainder of this section will be concerned with one fairly simple approach which also has considerable flexibility; that is, to subtract a running average from the data record. The average should be centered on the data point being operated upon. This process is essentially high-pass filtering, with a "turn-on" frequency determined by the averaging interval. The data of Figures 1 through 4 suggests that the background radiance level (basically interpreted to include gross ion-cloud radiance, sky brightness, and striation DC) occurs at much lower frequencies than the striations, so this simple subtraction process may provide satisfactory results.

* It will also be necessary to suppress the DC term required for physically meaningful radiance. That suppression is desirable for other reasons discussed later. If desired, the DC power can be added directly to the spatial frequency power spectra.

A Cautionary Note

A literal high-pass filter applied to the Fourier transform will not give equivalent results to those obtained using the subtraction process. We are working with sampled, digitized records of finite length. In consequence, the numerical Fourier transform at each frequency contains a contribution from all other frequencies. The numerical transform is the convolution of ideal transform and a sinc-function* corresponding to the length of the data set. The sinc-function propagated by DC will affect all higher frequencies and may, in fact, dominate the power spectrum (as is discussed further herein).

The effect of the convolution occurs simultaneously with the transform. It cannot be unfolded. If high frequency data has been modified substantially, a high-pass filter cannot retrieve the ideal data.

Basically, what we are doing is writing the total signal $N(x)$ as the sum

$$N(x) = B(x) + S(x)$$

of a nonstationary background, $B(x)$, which is of little or no interest, and a dc suppressed striation term, $S(x)$, which we hope to treat as ergodic. For a single record, the Fourier transform is

$$\tilde{N}(\omega) = \tilde{B}(\omega) + \tilde{S}(\omega)$$

so that the ideal power spectrum is

$$P(N, \omega) = \tilde{N}(\omega)^* \tilde{N}(\omega) = P(B, \omega) + P(S, \omega) +$$

[cross terms in B and S]

* $\text{sinc}(x) = (\sin x)/x$

If B and S are disjoint in frequency space, the cross terms are identically zero. The ideal power spectrum of a single record would simply be the sum of the power spectra of B and S. Since, however, the actual spectrum contains a convolved sinc-function, it is not possible to simply separate $P(S, \omega)$ out.

On the other hand, a prescription can be given which hopefully separates B from S directly and which essentially guarantees that the resulting functions are frequency disjoint. Since $P(B, \omega)$ and $P(S, \omega)$ can be formed from the separated functions, it appears that no information on the total power spectrum of the record is lost. However, one is able to treat the interesting part, $P(S, \omega)$, separately.

3.3.1 Ergodicity of S(x)

Suppose, then, that the separation is effected. One must ask whether anything has been accomplished; that is, does the k-th record power spectrum $P_k(S, \omega)$ tell us anything about the power spectrum of striations as a general class. Once again, the answer isn't clear. It depends on whether some apparently reasonable assumptions are correct.

If we assume that the radiance profiles of individual striations have the same form and that their location and amplitude are random, then it can be shown that the striation record waveform, S, is ergodic. And, in fact, if v is the striation ensemble average waveform, then

$$P(S, \omega) \propto P(v, \omega)$$

We must be careful in interpreting this expression since we are dealing with statistical quantities. Once the constant of proportionality, k, has been determined, $P(S)$ and $kP(v)$ are statistically indistinguishable. But that does not mean that they are numerically identical at each wavelength, ω . As the length of the record $s(x)$ increases, the statistics improve, which is to say the variance $[(P(S) - kP(v))^2]$ decreases. Only in the limit of an infinite record length is the variance of power estimates at each wavelength reduced to zero; thus, only in that limit is a numerical identity obtained. For records of

finite length, the variance of the estimate at each wavelength can be determined. Thus, the power spectrum of an ergodic record of finite length gives an estimate, with known variance, of the ensemble average power spectrum.

To illustrate how the constraint of proportionality is obtained, consider a restricted case of the above assumption in which the individual striation radiance profile amplitudes are fixed and identical. The striations, however, occur (replicate) with random spacing. Let the waveform to be replicated be $A(t)$. (In sketching the waveforms, $A(t)$ will be taken to be a square pulse. The formalism is general, however.) The Fourier transform of the replication element is $\tilde{A}(\omega)$ (Figure 9)

$$\tilde{A}(\omega) = \frac{1}{\sqrt{2\pi}} \int_{-\infty}^{\infty} A(t) e^{-i\omega t} dt$$

and is in general a complex quantity. The power spectrum of the waveform is

$$P_A(\omega) = \tilde{A}^*(\omega) \tilde{A}(\omega)$$

which is a real function of ω . The phase relations between the various wavelengths has been lost.

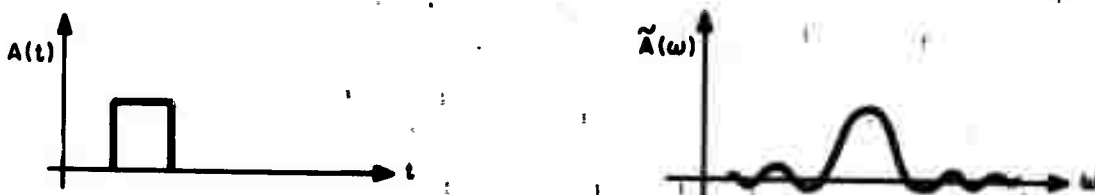


Figure 9. A single feature and its transform.

Now, let a replication of $A(t)$ occur at a later time. The waveform is $B(t)$. The total waveform is $A(t) + B(t)$, as illustrated in Figure 10. Since

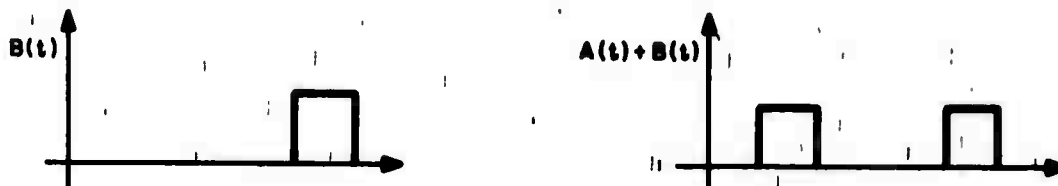


Figure 10. The addition of a second feature.

Fourier transformation is a linear process, the transform of the sum is

$$\widetilde{(A + B)} = \frac{1}{\sqrt{2\pi}} \int_{-\infty}^{\infty} (A(t) + B(t)) e^{-i\omega t} dt = \widetilde{A}(\omega) + \widetilde{B}(\omega)$$

Because $A(t)$ and $B(t)$ do not occur at the same time, $\widetilde{A}(\omega)$ and $\widetilde{B}(\omega)$ are not identical. However, since A and B are identical except for the time of occurrence, one expects \widetilde{A} and \widetilde{B} to be related, and in fact they are. Note that

$$B(t) = A(t - t_1)$$

where t_1 is the time between identical portions of the waveforms (e. g., the leading edge of a pulse). Now:

$$\widetilde{B}(\omega) = \frac{1}{\sqrt{2\pi}} \int B(t) e^{-i\omega t} dt = \frac{1}{\sqrt{2\pi}} \int A(t - t_1) e^{-i\omega t} dt$$

and letting $t' = t - t_1$ so that $dt = dt'$

$$\begin{aligned} \widetilde{B}(\omega) &= \frac{1}{\sqrt{2\pi}} \int A(t') e^{-i\omega t'} e^{-i\omega t_1} dt' \\ &= \frac{1}{\sqrt{2\pi}} e^{-i\omega t_1} \int A(t') e^{-i\omega t'} dt' \end{aligned}$$

or

$$\widetilde{B}(\omega) = \widetilde{A}(\omega) e^{-i\omega t_1}$$

Thus, the transforms of B and A are identical apart from phase factors. Clearly then, if the total waveform, $Z(t)$, consists of replication of $A(t)$ at times characterized by t_1, t_2, \dots, t_η (see Figure 11).

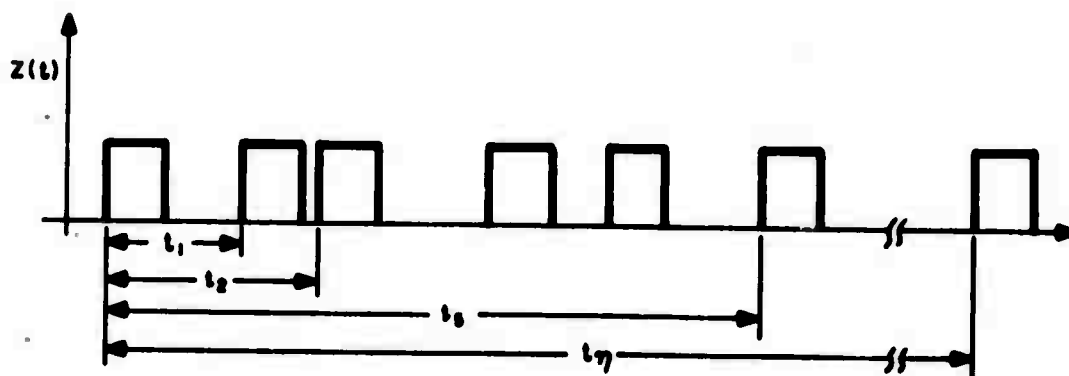


Figure 11. The total record of randomly replicated features.

The transform is

$$\tilde{Z}(\omega) = \tilde{A}(\omega) [1 + e^{-i\omega t_1} + e^{-i\omega t_2} + \dots + e^{-i\omega t_\eta}]$$

and the power spectrum of $Z(t)$

$$\tilde{Z} * \tilde{Z} = \tilde{A} * \tilde{A} [1 + e^{-i\omega t_1} + e^{-i\omega t_2} + \dots + e^{-i\omega t_\eta}]$$

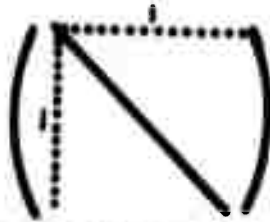
$$[1 + e^{i\omega t_1} + e^{i\omega t_2} + \dots + e^{i\omega t_\eta}]$$

$$= \tilde{A} * \tilde{A} \left(\sum_{j=0}^N e^{-i\omega t_j} \right) \left(\sum_{i=0}^N e^{i\omega t_i} \right)$$

where we have defined $t_0 = 0$ so that $e^{\pm i\omega t_0} = 1$. Since the sums are over different indices

$$\tilde{Z} * \tilde{Z} = \tilde{A} * \tilde{A} \left[\sum_{j=0}^N \sum_{i=0}^N e^{i\omega(t_j - t_i)} \right]$$

We can consider that the sum is over a two-dimensional array of the $\{t_i, t_j\}$, where, for instance, "i" is a column index and "j" a row index.



Break the double sum into three pieces, one piece consisting of all terms on the diagonal, the second all terms above the diagonal, and the third all terms below the diagonal

$$\begin{aligned} \tilde{Z}^* \tilde{Z} = \tilde{A}^* \tilde{A} & \left[\sum_{i=j=0}^N e^{-i\omega(t_j - t_i)} + \sum_{\substack{i>j \\ j=0}}^N e^{-i\omega(t_j - t_i)} \right. \\ & \left. + \sum_{\substack{i<j \\ j=0}}^N e^{-i\omega(t_j - t_i)} \right] \end{aligned}$$

Each element of the first \sum is identically 1, and the second and third terms are complex conjugates. Thus

$$\tilde{Z}^* \tilde{Z} = \tilde{A}^* \tilde{A} \left[N + 2 \operatorname{Re} \sum_{\substack{j>i \\ j=0}}^N e^{-i\omega(t_j - t_i)} \right]$$

$$\tilde{Z}^* \tilde{Z} = \tilde{A}^* \tilde{A} \left[N + 2 \sum_{\substack{j>i \\ i=0}}^N \cos \omega(t_j - t_i) \right]$$

To this point, the derivation is rigorous. If the time at which the replications occur is random, the argument of the cosine is also random. If N is large enough, one expects to see as many negative terms as positive terms in the remaining summation. Thus, if N is large enough, the remaining summation goes to zero and

$$\lim_{N \text{ large}} \tilde{Z}^* \tilde{Z} = N \tilde{A}^* \tilde{A}$$

In words, if enough randomly spaced replications are included, the power spectrum of the total waveform is simply N -times the spectrum of a replication unit.

To complete the analysis, consider that the real waveform consists of randomly timed replications of $A(t)$ plus some other signal $C(t)$:

$$Z(t) = C(t) + \sum_{i=0}^N A(t - t_i)$$

Then

$$\tilde{Z}(\omega) = \tilde{C}(\omega) + \tilde{A}(\omega) \left(\sum_{i=0}^N e^{-i\omega t_i} \right)$$

and

$$\tilde{Z}^* \tilde{Z} = \tilde{C}^* \tilde{C} + N \tilde{A}^* \tilde{A} + \tilde{C}^* \tilde{A} \sum_{i=0}^N e^{-i\omega t_i} + \tilde{C} \tilde{A}^* \sum_{j=0}^N e^{+i\omega t_j}$$

The last two terms are complex conjugates, and their total contribution is just twice the real part of either term. In this case, it is not possible to write the real part in a simple form; however, it is possible to write a

superficially simpler form as a basis to argue that the term is negligible.

Let

$$\tilde{D} = \tilde{C}^* \tilde{A} = d + i\delta \quad \text{and} \quad \tilde{G} = \sum_i e^{-i\omega t_i} = g + i\alpha,$$

then the last two terms contribute

$$2\text{Re } \tilde{D} \tilde{G} = 2(dg + \delta\alpha)$$

since

$$g = \sum \cos \omega t_i \approx 0$$

and

$$\alpha = \sum \sin \omega t_i \approx 0$$

By the same argument, the last terms are negligible to first order and

$$\tilde{Z}^* \tilde{Z} = \tilde{C}^* \tilde{C} + N \tilde{A}^* \tilde{A}$$

In words, the power spectrum of a waveform containing, among other things, N randomly spaced replications of a particular signal $A(t)$ will contain (to first order) N -times the power spectrum of A .

The more general assumption which we wish to make about striations is that the amplitude is also a random variable. (This is sometimes termed "Impulse Noise".) In that case, $S(x)$ is the sum of many similarly shaped transient pulses (see Figure 12).

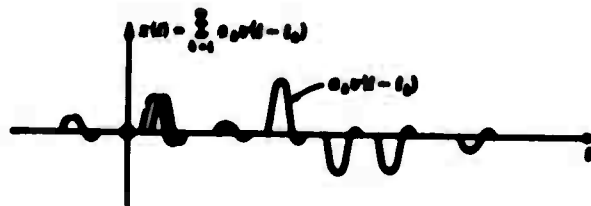


Figure 12. Sample functions $x(t)$ for five examples of random processes.

$$S(x) = \sum_{k=1}^{\infty} a_k v(x - x_k)$$

whose shape is given by $v = v(x)$, with

$$\int_{-\infty}^{\infty} v(x) e^{-iwx} dt = V(w)$$

while the pulse amplitude a_k is a random variable with finite variance, and the x 's are random locations determined by the state changes of a Poisson process with mean count rate α . The process is stationary and ergodic if started at $x = -\infty$; one has

$$\mu = E\{S(x)\} = \alpha E\{a_k\} \int_{-\infty}^{\infty} v(x) dt$$

$$R_S(x) = \mu + \alpha E\{a_k\} \int_{-\infty}^{\infty} v(x) v(x+1) dt$$

$$P(S, \omega) = \mu \delta(\omega) + \frac{\alpha}{2\pi} E\{a_k\} |V(\omega)|^2$$

where $E(u)$ denotes the expected value of u .

APPENDIX A
RADIOMETRIC INTERPRETATION
OF
PHOTOGRAPHIC RECORDS

A.1 INTRODUCTION

These notes present a brief outline of the mathematical formalism and the concepts used by EG&G to obtain source radiance and power information from photographic records. The notes were prepared during the 1971 SECEDE Summer Study.

A.2 BASIC CONCEPT

Radiometric interpretation of photographic records is based on the assumption that the measured density of an element of film is a monotonic function of the effective exposure, as defined by Eqs. (1) and (2), provided that other variables which affect density are held constant (e.g., exposure duration, processing, etc.). Therefore, if a calibration curve (a D-log E curve) is generated by measuring the densities, D_1 , of known exposures, E_1 , on film of the same emulsion as (and processed with) the data film, the effective exposure on the data film, $E_1(x, y)$, associated with a measured density, $D_1(x, y)$, may be obtained from this curve.

A.3 DENSITY DETERMINATION

Density measurements may be made with any of the several commercially available microdensitometers, with the understanding that calibration densities, D_1 , and image densities, $D_1(x, y)$, be measured with the same microdensitometer, using the same optics, and as close together in time as is feasible. This will eliminate all problems created by specular

versus diffuse measurements, and reduces the measurement to a comparison one in which the calibration and image densities are used only as transfer measurements of exposure.

A.4 CALIBRATION PROCEDURE

A.4.1 Step Wedge Exposure

As a minimum, each data record should receive four step-wedge exposures in a calibrated sensitometer (two pre-shot and two post-shot), with each pair placed head-to-head. Sensitometer exposure times should be chosen to most nearly correspond to data film exposure times. The step wedge exposures should be processed at the same time as, and adjacent to, the associated film record.

A.4.2 D-Log E Curve

The effective exposure, E_i , for the i^{th} step of the step wedge is taken to be

$$E_i = \int_0^{\infty} u(\lambda) T_i(\lambda) S(\lambda) d(\lambda) \quad \frac{\text{ergs}}{\text{cm}^2} \quad (1)$$

where

$u(\lambda)$ = spectral energy density on the sensitometer platen (ergs/cm²-Å),

$T_i(\lambda)$ = dimensionless diffuse transmittance of the i^{th} step, and

$S(\lambda)$ = dimensionless film sensitivity.

EG&G generally scans each of the four step wedges three times along parallel paths to produce twelve sets of density data (thirty-six for color film). Trial D-log E curves are constructed for each of the twelve scans, and these are reviewed in order to make adjustments and to eliminate

inconsistent data. A final D-log E curve is generated as an arithmetic mean of the acceptable trail curves.

A. 5 RADIANCE, POWER, AND ENERGY EQUATIONS

A. 5. 1 Radiance

For an imaging optical system focused at infinity, the effective exposure at (x, y) on the film is given by*

$$E_I(x, y) = \frac{10^7 \pi t_{\text{exp}}}{4 (f/)^2} \int_0^\infty N(\lambda) S(\lambda) T(\lambda) d\lambda \quad \frac{\text{ergs}}{\text{cm}^2} \quad (2)$$

where

$N(\lambda)$ = spectral radiance of point (X, Y) in the object plane corresponding to point (x, y) in the image plane (watts/cm²-ster-Å),

$T(\lambda)$ = the total spectral transmittance along the optical path,

$(f/)$ = the aperture of the optical system (focal length divided by the diameter of the lens aperture), and

t_{exp} = the exposure time at point (x, y) (seconds).

To unfold Eqn. (2) for $N(\lambda)$, assume that the relative shape, $\hat{N}(\lambda)$, of $N(\lambda)$ is known but not its magnitude, N_0 . Then,

$$N(\lambda) = N_0 \hat{N}(\lambda), \quad (3)$$

and Eqn. (2) yields

$$N(\lambda) = \frac{10^{-7} 4(f/)^2}{\pi t_{\text{exp}}} \frac{\hat{N}(\lambda)}{\int_0^\infty \hat{N}(\lambda) T(\lambda) S(\lambda) d\lambda} E_I(x, y). \quad (4)$$

* Eqn. (2) assumes that the source area considered is on or near the optical axis.

The total radiance in the wavelength range (a, b) is then

$$\begin{aligned}
 N_{ab}(X, Y) &= \int_a^b N(\lambda) d\lambda \\
 &= \frac{10^{-7} 4(f/l)^2}{\pi t_{\text{exp}}} \frac{\int_a^b \hat{N}(\lambda) d\lambda}{\int_0^\infty \hat{N}(\lambda) T(\lambda) S(\lambda) d\lambda} E_I(x, y) \frac{\text{watts}}{\text{cm}^2 \text{-ster}} \quad (5)
 \end{aligned}$$

Note that $T(\lambda)$ may be written as

$$T(\lambda) = T_A(\lambda) T_W(\lambda) T_F(\lambda) T_P(\lambda) T_L(\lambda), \quad (6)$$

where

- $T_A(\lambda)$ = spectral transmittance of the atmosphere,
- $T_W(\lambda)$ = spectral window transmittance,
- $T_F(\lambda)$ = spectral filter transmittance,
- $T_P(\lambda)$ = spectral prism transmittance, and
- $T_L(\lambda)$ = spectral lens transmittance.

For black and white film, the limits of integration (a, b) are usually 3800 - 6800 Å. For color film, each layer is treated separately, with the limits usually taken as 3800 - 4800 Å, 4300 - 5800 Å, and 5800 - 6800 Å.

A. 5. 2 Power

Assume that the radiating source is located on the optical axis and that its dimensions are small compared to the distance between the source and the camera. Then, if the source is (1) an optically thin volume rather or (2) a spherical Lambert surface radiator, the total radiated power in the wavelength interval (a, b) is given by

$$P_{ab} = 4\pi \int_X \int_Y N_{ab}(X, Y) dX dY \quad (7)$$

or,

$$P_{ab} = 4\pi \left(\frac{ROA}{FL} \right)^2 \int_x \int_y N_{ab}(X, Y) dx dy \quad \text{watts} \quad (8)$$

where the integration is performed over a designated area of the film (perhaps the entire frame), and

ROA = range along the optical axis and

FL = lens focal length.

Once $N_{ab}(X, Y)$ has been evaluated from Eqn. (5), P_{ab} may be calculated from Eqn. (8). When the above assumptions do not hold, special calculation procedures must be followed.

A. 5.3 Total Energy

Through a consideration of successive frames of a record, the time dependence of P_{ab} may be determined. Thus, the total radiated energy in the range (a, b) and in the time interval $(t_2 - t_1)$ may be written as

$$U_{ab} = \int_{t_1}^{t_2} P_{ab}(t) dt \quad \text{joules.} \quad (9)$$

Equations (5), (8), and (9) are the basic equations employed in obtaining radiometric information from photographic records.

A. 6 FACTORS IN THE EQUATIONS

A. 6.1 Exposure Time

The exposure time (t_{exp}) should be measured directly or computed from measurements of film velocity and camera characteristics.

A. 6.2 Lens Spectral Transmittance/Optical Aperture

EG&G obtains the lens spectral transmittance ($T_L(\lambda)$) from measurements of the actual lens at the nominal setting. The curve thus generated is not the true spectral transmittance of the lens, but includes any differences between the nominal $f/$ and the effective $f/$. The curve

generated is

$$T_L(\lambda) = T_1(\lambda) \frac{(f/)^2_{\text{nominal}}}{(f/)^2_{\text{effective}}},$$

where $T_1(\lambda)$ is the true spectral transmittance of the lens. The nominal $f/$ is used in the radiance equation.

A. 6.3 Atmospheric Spectral Transmittance

The atmospheric spectral transmittance ($T_A(\lambda)$) can be a unique quantity for each photograph. Ideally, measurements of $T_A(\lambda)$ should be made for each exposure, or, since this is almost an impossible task, a mathematical model of atmospheric transmission can be constructed so that $T_A(\lambda)$ can be calculated as both a spectrally and spatially varying quantity.

A. 6.4 Spectral Transmittances

The several spectral transmittances used in Eqns. (5) and (6) should all be measured values.